Development of GPC2-directed chimeric antigen receptors using mRNA for pediatric brain tumors

Jessica B. Foster,[1,2] Crystal Griffin,[3] Jo Lynne Rokita,[3-5] Allison Stern,[3] Cameron Brimley,[5] Komal Rathi,[3,4] Maria V. Lane,[1] Samantha N. Buongervino,[1] Tiffany Smith,[3] Daniel Martinez,[6] Robert Weschler-Reya,[7] Katalin Karikó,[8] Phillip B. Storm,[3,5] David M. Barrett,[9] Adam C. Resnick, [3,5] John M. Maris,[1,2] Kristopher R. Bosse[1,2]

[1] Division of Oncology, Children's Hospital of Philadelphia, Philadelphia, PA, USA
[2] Department of Pediatrics, Perelman School of Medicine at the University of Pennsylvania; Philadelphia, PA, USA
[3] Center for Data-Driven Discovery in Biomedicine, Children's Hospital of Philadelphia, Philadelphia, PA, USA
[4] Department of Bioinformatics and Health Informatics, Children's Hospital of Philadelphia, Philadelphia, PA, USA
[5] Division of Neurosurgery, Children's Hospital of Philadelphia, Philadelphia, PA, USA
[6] Division of Pathology, Children's Hospital of Philadelphia, Philadelphia, PA, USA
[7] Sanford Burnham Prebys Medical Discovery Institute, San Diego, CA, USA
[8] BioNTech, Mainz, Germany
[9] Tmunity Therapeutics, Philadelphia, PA, USA

Corresponding author:
Jessica Foster, MD
3501 Civic Center Blvd
CTRB Room 3052
Philadelphia, PA 19104
fosterjb@chop.edu
267-425-1918

Keywords: glypican, chimeric antigen receptor, pediatric brain tumor, immunotherapy

Conflict of Interest: T.S. is currently employed by Spark Therapeutics. K.K. is currently employed by BioNTech. D.M.B. is currently employed by Tmunity Therapeutics. J.B.F., D.M.B, J.M.M., and K.R.B. hold patents for the discovery and development of immunotherapies for cancer, including patents related to GPC2-directed immunotherapies. K.R.B. and J.M.M. receive research funding from Tmunity for research on GPC2-directed immunotherapies and J.B.F., D.M.B, J.M.M., and K.R.B. receive royalties from Tmunity for licensing of GPC2-related intellectual property. All other authors have nothing to disclose.

Abstract

Pediatric brain tumors are the leading cause of cancer death in children with an urgent need for innovative therapies. Here we show that the neuroblastoma cell surface oncoprotein glypican 2 (GPC2) is also highly expressed on multiple lethal pediatric brain tumors, including medulloblastomas, embryonal tumors with multi-layered rosettes, other CNS embryonal tumors, as well as a subset of highly malignant gliomas including H3 G35 mutant gliomas and some H3 K28M diffuse midline gliomas. To target GPC2 on these pediatric brain tumors with adoptive cellular therapies and to mitigate potential inflammatory neurotoxicity, we developed four mRNA chimeric antigen receptor (CAR) T cell constructs using the highly GPC2-specific, fully human D3 scFv that targets a conformational epitope on human and murine GPC2. First, we validated and prioritized these GPC2-directed mRNA CARs using *in vitro* cytotoxicity and T cell degranulation assays with GPC2-expressing neuroblastoma cells. Next, we expanded the testing of the two most potent GPC2-directed CAR constructs (D3V3 and D3V4) prioritized from these studies to GPC2-expressing medulloblastoma and high-grade glioma models, showing significant GPC2-specific cell death in multiple medulloblastoma and HGG cellular models. Finally, locoregional delivery of both GPC2-directed mRNA CAR T cells induced significant and sustained tumor regression in two orthotopic medulloblastoma models, and significantly prolonged survival in an aggressive orthotopic thalamic diffuse midline glioma model. No GPC2-directed CAR T cell related neurologic or systemic toxicity was observed. Taken together, these data show that GPC2 is a highly differentially expressed cell surface protein on multiple malignant pediatric brain tumors that can be targeted safely with local delivery of mRNA CAR T cells.

Introduction

Immunotherapy has developed into a major paradigm for the treatment of cancer over the past two decades[1]. Chimeric antigen receptor (CAR) T cells are one form of immunotherapy, where targeted T cell killing is achieved through combining the specificity of an antibody with the stimulatory signals of cytotoxic T cells[2]. CAR T cell therapy has provided dramatic success in leukemias and lymphomas[3-5], and tisagenlecleucel recently became the first FDA approved cellular therapy product[6]. This excitement has prompted similar investigations for solid tumors but without significant success to date[7]. Developing effective CAR T cell therapy for solid tumors has many challenges related to difficulty finding appropriate target antigens, the suppressive tumor microenvironment, T cell dysfunction, and poor CAR T cell trafficking[7]. Among brain tumors, CAR T cell therapy remains in its infancy, with a handful of adult clinical trials showing minimal to transient success[8-10], and trials in pediatric brain tumors only just beginning.

The majority of CAR T cell work to date has used viral vectors to produce constitutively expressed CAR molecules[11]. However, CAR molecules may also be introduced into T cells using *in vitro* transcribed mRNA[12], and we have shown effective CAR T cells can be made utilizing the same innovative technology that recently allowed mRNA to be successfully employed for COVID-19 vaccination development[13,14]. Using mRNA to generate CAR T cells for adoptive transfer may offer several advantages in the clinic or in preclinical validation of CARs. First, mRNA transfection is a more efficient process than viral transduction, with uniformly high levels of CAR on the surface[15]. Second, due to the quicker production time, iterative changes in the CAR binding site or structure are more easily tested[16]. Third, mRNA is

less expensive than viral vectors when scaling up to clinical grade application. Finally, when exploring novel immunotherapeutic targets, transient expression may be desirable to ensure safety, particularly in the brain where off-target toxicity may cause significant morbidity and mortality[17]. The major disadvantage of using mRNA CAR T cells is the transient nature, which may not offer the persistence needed for full eradication of disease[16]. Prior work has shown that while systemic delivery of mRNA CAR T cells does not result in long term disease control[18-20], local delivery into solid tumors can be remarkably effective[21,22].

We have recently shown that Glypican 2 (GPC2) is a heparan-sulfate proteoglycan cell-surface oncoprotein that is overexpressed on the surface of neuroblastomas as well as several other pediatric and adult cancers[23,24]. GPC2 appears to harbor all the qualities of a bona fide immunotherapeutic target, including cell-surface location, tumor-specific expression, tumor dependence and enrichment in the tumor stem cell compartment[23,24]. To therapeutically capitalize on this differential expression, we and others have identified several GPC2-specific binders[23,25,26] and shown robust efficacy of GPC2-targeting antibody-drug conjugates (ADCs)[23,24], immunotoxins[25], and DNA vector-derived CAR T cells[25,26]. Here we sought to build upon these data with a specific focus on GPC2 in pediatric brain cancers, both in better defining the brain tumor histotypes that harbor high-levels of GPC2 expression and in creating GPC2-redirected mRNA CAR T cells to enable a safe and efficacious therapeutic approach for local intracranial delivery.

Results

GPC2 is expressed in multiple pediatric brain tumors and correlated with MYCN expression and chromosome 7q gain

GPC2 is a differentially expressed MYCN-regulated oncoprotein found on the surface of most neuroblastomas and several other embryonal cancers, including medulloblastomas and retinoblastomas[23,24]. To better define *GPC2* expression specifically in pediatric brain tumors, we analyzed RNA sequencing data from 20 unique pediatric CNS tumor types (total n=833) in the Pediatric Brain Tumor Atlas (OpenPBTA), which revealed that several additional pediatric CNS tumors harbor high-levels of *GPC2* RNA (**Fig 1A**). Based on normal expression data from the Genotype-Tissue expression (GTex) portal, we chose a cutoff value of a TPM of 10 to delineate high *GPC2* expression. Evaluation of tumors throughout the OpenPBTA biorepository showed high *GPC2* expression in 100% of embryonal tumors with multilayered rosettes (ETMR), 95% of medulloblastomas, 93% other CNS embryonal tumors (CNS embryonal tumor, NOS), 50% of choroid plexus carcinomas (CPC), 41% of high-grade gliomas (HGG) without H3K28M mutation, and 40% of diffuse midline gliomas (DMG) (**Fig 1B**). While several tumor histotypes were uniform in their *GPC2* expression levels, multiple subtypes had significant heterogeneity in *GPC2* expression motivating us to look further at *GPC2* expression across tumor molecular subgroups where possible. First, for medulloblastomas, we observed the highest *GPC2* expression in group 4 compared to the other subtypes (Wnt, SHH, and group 3; $p<0.01$) (**Fig 1C, left**), consistent with our prior results[23]. Across high grade glioma subgroups, H3 G35 mutant gliomas had the highest *GPC2* expression ($p<0.05$; **Fig 1C, middle**). Embryonal tumors showed high expression across all subgroups (**Fig 1C, right**).

We have also previously found that significantly higher levels of *GPC2* expression are found in neuroblastoma or medulloblastoma tumors that harbor either high level expression of a MYC gene family member and/or contain somatic gain of the *GPC2* locus on chromosome 7q[23]. To determine if similar drivers to *GPC2* expression are present across this diverse set of pediatric brain tumors we stratified tumors by chromosome 7q copy number and found that 6.7% of tumors had 7q gain (38 of 565 tumors with copy number data available). The majority of those were medulloblastoma (n=14), LGG (n=8) and HGG (n=7) (**Fig 1D**). Those tumors with 7q gain showed significantly higher *GPC2* expression ($p<0.0001$; **Fig 1E, left**). This chromosome 7q gain and increased *GPC2* expression correlation was also found in medulloblastomas ($p<0.05$) **(Fig 1E, center)**, and the same trend was found in high grade gliomas but was not statistically significant (**Fig 1E, right**). Furthermore, we also observed a positive correlation between *GPC2* and *MYCN* expression within this pediatric brain tumor dataset ($r=0.3073$, $p<0.0001$; **Fig 1F, top**), suggesting that MYCN may also regulate *GPC2* expression in some pediatric brain tumors as well. This *MYCN/GPC2* expression correlation was robust in high grade gliomas ($r=0.524$, $p<0.0001$; **Fig 1F, middle**), but this correlation was not found in medulloblastoma ($r=0.16$, p=ns; **Fig 1F, bottom**).

Next, to evaluate if *GPC2* expression is maintained at the time of brain tumor relapse, we evaluated 47 unique patients with paired diagnosis-relapse tumor RNA sequencing data, including 7 patients with multiple relapsed tumor specimens (**Fig 1G**). *GPC2* expression was generally similar at the time of diagnosis and relapses across all brain tumor histotypes. Looking specifically at medulloblastomas and HGGs, again *GPC2* expression was generally

stable, however with individual cases showing both increases and decreases in *GPC2* expression at the time of relapse (**Fig 1G, bottom**).

OpenPBTA data generation is completed on patient samples provided through the Children's Brain Tumor Network (CBTN). The CBTN also performs cell line generation both in serum-free media and media containing fetal bovine serum (FBS). For ten HGG primary tumors, cell lines have been generated in both media types, with subsequent transcriptome profiling with RNA sequencing, providing the opportunity to compare *GPC2* expression in these paired *in vitro* models.[27] *GPC2* expression was increased in HGG cell lines generated in serum-free conditions ($p<0.01$; **Fig 1H**). This increase in *GPC2* expression mirrored the expression trends of other neuronal stem cell markers Olig2, SOX2, and CD133 (**Fig 1H**), suggesting that serum-free conditions better propagate stem-like cells from tumors[28,29] and that *GPC2* expression is increased in the HGG stem cell compartment, similar to what we have previously described in neuroblastomas and small cell lung cancers[24].

Finally, we next looked to validate these RNA data by quantifying GPC2 expression in a subset of pediatric brain tumors using immunohistochemistry (IHC), flow cytometry, and western blot. First, we evaluated GPC2 expression by IHC, utilizing a HGG-focused tumor microarray which includes 73 HGGs (glioblastomas, anaplastic astrocytomas, and DMGs), as well as 6 CNS embryonal tumors NOS, 4 medulloblastomas, 3 pineoblastomas, 2 ETMRs, 2 ependymomas, 2 ATRTs, 1 high-grade neuroepithelial tumor with BCOR alteration (HGNET-BCOR), 1 oligodendroglioma, and 1 LGG. Most of the HGG tumors harbored positive GPC2 staining (**Fig 2A**), with very strong staining in the single H3 G35 mutant tumor included in the array (**Fig 2B**).

In addition, strong GPC2 staining was also observed in 2 out of 4 medulloblastomas, 1 of 2 ETMRs, 2 of 3 pineoblastomas, 1 of 1 HGNET-BCOR, and 2 of 6 embryonal tumors NOS (**Fig 2B**). GPC2 flow cytometry of medulloblastoma (n= 4) and HGG (n=6) cell lines confirmed robust GPC2 cell-surface expression comparable to the neuroblastoma cell line SMS-SAN (**Fig 2C, D).** Of note the two cell lines with the highest GPC2 cell surface expression were a group 4 medulloblastoma (7316-4509) and a H3 G35 HGG (7316-158), consistent with transcriptomic profiling and IHC. Finally, total GPC2 protein expression in medulloblastoma and HGG cell lines by Western blotting was also found to be comparable to the SMS-SAN neuroblastoma cell line (**Fig 2E**). Taken together, these data show that GPC2 is highly expressed on a cohort of malignant pediatric brain tumors, supporting the testing of GPC2 immune-based therapies in these lethal childhood CNS tumors.

mRNA GPC2 CAR T cells are cytotoxic to GPC2-expressing neuroblastoma and brain tumor cell lines

For GPC2 CAR generation, we used the single chain variable fragment (scFv) portion of the D3 GPC2 antibody[23,24] that binds a conformational epitope of the GPC2 extracellular domain that is identical between human and murine. We explored four different configurations of the D3 scFv by manipulating the orientation of the heavy and light chains, as well as the glycine-serine linker length between the heavy and light chains (5 versus 15 amino acids), to identify the structure that provided optimal CAR expression, cell killing, and T cell activation (**Fig 3A)**. All four constructs included a CD8 hinge and transmembrane domain with 41BB costimulatory domain and CD3ζ signaling. CAR mRNA was *in vitro* transcribed and transfected into human T cells, and after 24 hours we evaluated CAR expression and binding to GPC2 via incubation

with GPC2-PE. All four constructs showed GPC2 specific binding compared to GD2-directed CAR control (mean MFI 18,721 to 54,849 for constructs versus 684 for control, $p<0.001$) (**Fig 3B)**. Serial GPC2 CAR expression as measured by protein L flow cytometry showed that typically CAR expression persisted for 5-7 days (**Fig 3C**), with the D3V3 and D3V4 CARs having a modestly prolonged persistence with residual CAR expression at 7 days. To investigate T cell exhaustion, we also measured the expression of negative checkpoint regulators on the surface of GPC2 CAR transfected T cells and found no difference in checkpoint molecule expression across the 4 different constructs (**Fig 3D**).

We next evaluated the cytotoxicity of CAR T cell constructs *in vitro* using multiple well-characterized neuroblastoma cell lines with variable levels of GPC2 cell surface expression[23]. CAR T cells transfected with all 4 GPC2 CAR constructs were able to exert robust killing of the GPC2-high cell lines SKNAS-GPC2, SMS-SAN, and Nb-EbC1 ($p<0.0001$) (**Fig 4A**), with limited killing of GPC2 low expressing native SKNAS and control 293T cells (10:1 E:T; **Fig 4B**). However, at lower E:T ratios (5:1) there was differential cytotoxicity between GPC2 CARs with the D3V3 and D3V4 constructs performing superiorly, most notable on the NB-EbC1 cell line (**Fig 4A**). Furthermore, there was differential T cell activation across the 4 GPC2 CARs, with the D3V3 and D3V4 constructs showing the highest levels of interferon gamma (IFNγ) and interleukin 2 (IL-2) release by ELISA upon co-incubation with GPC2-high neuroblastoma cells ($p<0.0001$) (**Fig 4C**). Considering these data, the D3V3 and D3V4 GPC2 CAR constructs were prioritized for further testing in brain tumor models based on their superior persistence, *in vitro* cytotoxicity, and T cell activation.

We next tested the cytotoxicity of the prioritized D3V3 and D3V4 GPC2-directed CARs in a panel of medulloblastoma and HGG cell lines with different levels of GPC2 expression (**Fig 2D**), using real-time cell electronic sensing (RT-CES) assay for adherent cell lines (DAOY, 7316-913, and 7316-5335) and luciferase assays for suspension cell lines (7316-4509, 7316-3058, and 7316-24). GPC2-expressing brain tumor cells were selectively killed with GPC2 CAR T cells, but not the CD19 control CAR T cells at E:T ratios of 5:1 or higher ($p<0.0001$) (**Fig 5A and 5B**). GPC2-directed CAR T cells also showed significant IFNγ release in the presence of GPC2-expressing brain tumor cell lines compared to CD19-directed CAR T cells ($p<0.0001$) (**Fig 5C**).

mRNA GPC2-redirected CAR T cells induce sustained tumor regression and increased survival in pediatric brain tumor xenograft models

To evaluate the *in vivo* efficacy of the D3V3 and D3V4 mRNA GPC2-directed CAR T cells, we utilized medulloblastoma and DMG xenograft models. Given the shortened duration of activity with mRNA CAR T cells, and recent work on CAR T cells for CNS tumors reporting increased efficacy with locoregional delivery,[9,30] we focused on intratumoral delivery of the prioritized D3V3 and D3V4 GPC2 RNA CAR T cells. Following orthotopic tumor engraftment of 7316-4509 group 4 medulloblastoma in mice, we placed a fixed guide cannula into the tumor bed that would enable serial CAR T cell dosing, and treated mice with $4x10^6$ of either GPC2- or CD19-directed CAR T cells via catheter into the tumor bed twice a week for 2 weeks for a total of 4 doses. Both D3V3 and D3V4 CAR T cell constructs resulted in sustained 7316-4509 medulloblastoma tumor regression ($p<0.0001$; **Fig 6A**). We next treated the group 3 medulloblastoma Rcmb28 xenograft in an identical manner with $4x10^6$ of either D3V3 or D3V4

GPC2-directed or CD19-directed CAR T cells via catheter into the tumor bed twice a week for a total of 5 doses, which again showed sustained tumor control via bioluminescent imaging ($p<0.0001$; **Fig 6B**). For both models, tumor regression was also confirmed by IHC at study endpoint (**Fig 6C**). Notably, no evidence of clinical toxicity was observed in these animals, with no weight loss or neurologic toxicity, utilizing the CARs engineered from the D3 GPC2 antibody which binds equally the murine and human GPC2 protein[24].

As both the 7316-4509 and Rcmb28 medulloblastoma xenograft models developed clinical signs of graft versus host disease (GvHD) from repeated doses of human T cells prior to tumor end point, we next utilized the clinically aggressive, fast-growing thalamic DMG 7316-3058 xenograft model to evaluate the ability of mRNA GPC2-directed CARs to induce prolonged murine survival. Prior studies treating thalamic DMG xenograft murine models with GD2-directed CAR T cells has resulted in fatal pseudoprogression and hydrocephalus[31]. However, we hypothesized that serial low doses of GPC2 mRNA CAR T cells may avoid CNS toxicity due to their transient nature, but still provide tumor control. Using lower doses of 2×10^6 GPC2- or CD19-directed CAR T cells also allowed study observations up to 60 days post initial T cell infusion. CAR T cells were delivered intratumoral via catheter for a total of 6 doses, and D3V3 and D3V4 GPC2-directed CAR T cells both significantly prolonged murine survival compared to CD19 CAR T cell controls (median survival of 55 days for D3V3 GPC2 CARs and >60 days for D3V4 GPC2 CARs versus 33 days for CD19 CARs; $p<0.05$ and $p<0.01$, respectively) (**Fig 5C**). Again, no clinical toxicity was observed during the prolonged course of this study with these murine GPC2 cross-reacting CAR T cells.

Discussion

Pediatric brain tumors are the leading cause of death in the pediatric oncology clinic[32]. CAR T cells have transformed the treatment of relapsed and refractory leukemia and lymphoma, with continued pursuit for similar efficacy in solid and brain tumors. Our group recently identified GPC2 as a bona fide immunotherapeutic target in neuroblastoma with expression in other pediatric and adult tumors, demonstrating robust and sustained efficacy of a GPC2 ADC utilizing the GPC2 D3 antibody[23,24]. We and others have also shown that lentiviral-based GPC2 DNA CARs can lead to significant efficacy in neuroblastoma murine models utilizing alternative GPC2 scFvs[25,26]. Here we focus on GPC2 in pediatric brain tumors, both in quantifying GPC2 expression across a wide-range of unique brain tumor histotypes, and on developing mRNA-based GPC2-directed CARs to enable pediatric brain tumor treatment approaches. We describe the creation and manipulation of a CAR construct using the same D3 binding domain utilized in our prior GPC2 ADC work, to optimize performance in CAR T cells.

Investigation of GPC2 expression using RNA sequencing and various proteomic approaches revealed elevated GPC2 expression across diverse groups of pediatric brain tumors. While many of these pediatric brain tumors have embryonal phenotypes similar to neuroblastoma, such as medulloblastoma, ETMR, CNS embryonal tumors NOS, and pineoblastomas, several others do not share this phenotype, including HGG and CPC. H3 G35 mutant tumors showed the highest *GPC2* expression among HGGs, and have been shown to be driven by overexpression of MYCN[33]. CPC was also recently shown to be driven by activation of MYC paired with loss of TP53[34]. This increase in MYCN and MYC activity may account for the

increased *GPC2* expression in these groups, as we have previously shown MYC family proteins induce higher *GPC2* expression in neuroblastoma[23]. Across the CBTN cohort, *MYCN* expression was positively correlated with *GPC2* expression, although not in medulloblastoma. In medulloblastoma increased *GPC2* expression may be driven in part by 7q gain[23]. Future work will focus on understanding factors driving *GPC2* expression in all pediatric brain tumors, and identification of other drivers that may be contributing. Our data also show that GPC2 in HGG cell lines seems to coincide with a highly malignant stem-like population of cells and enhanced GPC2 expression could be selected for by using stem cell conditions in cell line development. This is consistent with our recent finding that GPC2 expression is increased in the stem cell compartment of neuroblastomas and small cell lung cancers[24], and future work will evaluate the potential oncogenic and stem-like properties of these cells in pediatric brain tumors. Our RNA sequencing data also showed no significant difference in *GPC2* expression across diagnosis-relapse paired samples, suggesting GPC2-directed CARs may be efficacious in both settings in the clinic.

Using mRNA we were able to develop multiple CAR T cell constructs from one scFv domain, D3, which was previously used successfully to create an ADC. Our data showed the light-to-heavy configuration of the scFv proved superior, with efficacy *in vivo* using both the 15 amino acid and 5 amino acid linker between the chains. This work was carried out using an mRNA CAR construct for two reasons. First, mRNA is more facile for quick iterative testing of different constructs. Unfortunately, evaluation of optimal configuration for CAR T cells remains empirical, with different targets requiring different adjustments for optimal efficacy. Our mRNA methodology[13] allowed for quick testing and prioritization of the D3V3 and D3V4 constructs,

and should be utilized for screening of other novel CAR constructs. Second, mRNA CAR T cells may mitigate any potential off-target toxicity when GPC2 CAR T cells are delivered to the brain given their transient CAR expression. In our aggressive thalamic DMG model, we were able to avoid fatal pseudoprogression as previously observed in other studies using viral-based CAR T cells targeting thalamic DMG[31], by employing serial low doses of mRNA GPC2-directed CAR T cells.

As previously described, mRNA CAR T cells have not been shown to effectively eradicate solid tumors via IV injection due to their transient nature[18]. However, intratumoral or local delivery can produce full tumor regression[18,21,22,35], which we have also shown here with our experiments using mRNA GPC2-directed CAR T cells in two medulloblastoma models and one thalamic DMG model. With growing evidence for the effectiveness of locoregional delivery of CAR T cells for brain tumors both preclinically[30,36,37] and in trials[9], the cannula system we developed for repeated CAR T cell delivery serves as an important platform for preclinical CAR T cell testing. The cannulas simulate an Ommaya reservoir, which is currently being used in ongoing clinical trials for CAR T cells in pediatric brain tumors (NCT03500991, NCT03638167, NCT04185038, NCT04196413), propelling the translational applicability of this work and providing a clinical platform for future studies in humans.

In conclusion, this work has shown that the immunotherapeutic target GPC2 is highly expressed across a variety of pediatric brain tumors, including malignant embryonal tumors (CNS embryonal tumors NOS, ETMRs, medulloblastomas) and a subset of HGGs and DMGs. Using mRNA we created two efficacious CAR constructs from the D3 binder and show efficacy

in several pediatric brain tumor preclinical models, laying the foundation for the translation of GPC2 CARs to pediatric brain tumors.

Methods

RNA sequencing of primary tumor samples and patient derived xenografts

RNA sequencing of pediatric brain tumor samples was completed as described within the OpenPBTA[38] (available at https://alexslemonade.github.io/OpenPBTA-manuscript/v/0d99c02483e21557e27957386d419b58fe8cb635/ or from the public CAVATICA project: https://cavatica.sbgenomics.com/u/cavatica/openpbta). Briefly, 1,028 paired-end RNA fastq files, comprising 970 rRNA-depleted and 58 poly-A enriched samples, were aligned to the hg38 human genome using GENCODE version 27 as reference annotation with STAR v2.6.1d. Gene level quantification in terms of TPM (transcripts per million) was quantified using RSEM version 1.3.1. The rRNA depleted and poly-A enriched samples were batch corrected using the ComBat function of R package sva.

Tumor Cell lines

Neuroblastoma cell lines were maintained in culture as previously described[23,39] with RPMI media supplemented with Penicillin/Streptomycin, L-glutamine, and 10% FBS. Brain tumor cell lines were maintained in serum free culture, using DMEM:F12 media supplemented with EGF, FGF and B27. Luciferase was introduced into pediatric brain tumor cell lines using lentiviral plasmids: pLenti CMV Puro LUC (w168-1) was a gift from Eric Campeau & Paul Kaufman[40] (Addgene plasmid # 17477 ; http://n2t.net/addgene:17477 ; RRID:Addgene_17477) and pLL-EF1a-rFLuc-T2A-GFP-mPGK-Puro (LL410PA-1, System Biosciences). Preparation and transduction was completed as previously described,[23] or with pre-made lentivirus expressing firefly luciferase with GFP (PLV-10173-200, Cellomics). Cell lines were tested for mycoplasma and confirmed with STR sequencing.

T cell expansion and transfection

Human T cells from healthy de-identified donors were purchased from the University of Pennsylvania Immunology Core and stimulated with CD3/CD28 beads (11131D, Gibco) as previously described[41]. Stimulated and rested T cells were frozen in liquid nitrogen prior to use. After thawing and resting for one day, transfection was completed using Amaxa Nucleofector (Lonza) or ECM 830 (BTX) electroporation systems as previously described[13].

CAR construct cloning

Sequences encoding the D3 scFV were combined with sequences encoding a CD8 hinge and transmembrane domain, followed by 41BB and CD3ζ co-stimulatory domains, to create the CAR constructs. CAR plasmids were generated by GenScript, and then cloned into a pTEV vector backbone (generous gift of Dr. Katalin Karikó) using Geneart Seamless cloning (A14603, Invitrogen).

In vitro mRNA synthesis

mRNA encoding CAR constructs were synthesized from the pTEV vectors using Megascript T7 transciption kit (AM1334, Invitrogen) and replacing UTP with N-methyl pseudouridine (N-1081, TriLink Biotechnologies) as previously described[13]. After synthesis, all mRNA was purified with RNase III (RN02950, Epicenter), followed by capping and tailing as previously described[13].

Western blot validation of protein expression

Tumor cell lines were lysed and western blotting completed as previously described[23], using anti-Glypican-2 (1:500; F-5, sc-393824, Santa Cruz Biotechnology) for protein detection.

Flow cytometry

Flow cytometry was performed on tumor cell lines to confirm GPC2 expression on the cell surface. Tumor cell lines were washed in FACS buffer (500 mL PBS, 10 mL FBS, 2 mL 0.5 M EDTA), then incubated in D3-GPC2-IgG1 conjugated to phycoerythrin (PE) at 1:800 for 20 minutes in the dark at 4° C. Conjugation with PE was completed using conjugation kit (ab102918, Abcam). For quantification of surface GPC2, BD Quantibrite beads (340495, BD Biosciences) were used per manufacturer's instruction.

CAR T cell constructs were evaluated for GPC2 specific binding by staining with GPC2 protein (R&D) conjugated to PE. CAR T cells were washed in FACS buffer and incubated in GPC2-PE at 1:100 for 20 minutes in the dark at 4° C, and then washed again in FACS buffer before analysis. CAR T cells were evaluated for CAR expression on the surface by flow cytometry with protein L (1:100; M00097, Genscript) as previously described[42]. Flow cytometry for negative checkpoint regulator was performed as previously described[13] using antibodies: BV510 mouse anti-human CD279 (PD1) (1:100; 563076, BD Horizon), PerCP-eFluor 710 mouse anti-human CD223 (LAG-3) (1:100; 46-2239-41, Invitrogen), and BV421 mouse anti-human CD366 (TIM-3) (1:100; 565562, BD Biosciences).

Flow cytometry data was acquired on BD Accuri C6 (BD Biosciences) or FACS Verse (BD Biosciences) flow cytometers. Analysis was completed on FlowJo 10.2 (Treestar).

Cytotoxicity assays

Measurement of CAR T cell dependent tumor cell killing was measured by several methods. For adherent tumor cell lines, cell proliferation was measured using Real-time Excelligence system (RT-CES, F Hoffman La-Roche) measured every hour. For suspension cell lines, luciferase containing tumor cells were plated in 96 well plate, CAR T cells plated after 24 hours, and Bright Glo luciferase assay (E2620, Promega) was run after 48 hours of co-incubation. CAR T cells were plated in at least triplicate on tumor cells at E:T ratios of 10:1, 5:1 and 1:1. Each experiment was repeated at least two times.

CAR T Cell cytokine release

Tumor specific CAR T cell degranulation was determined using ELISA to detect interferon-gamma and IL-2. Tumor cells and CAR T cells were plated as described above and allowed to co-incubate for 24-48 hours. Plates were then spun and supernatant collected for evaluation using human IL-2 duoset ELISA (DY202, R&D) and human IFN-gamma duoset ELISA (D285B, R&D) per manufacturer's instructions.

Mouse studies

In vivo studies were completed in mice under an approved protocol by the Institutional Animal Care and Use Committee of the Children's Hospital of Philadelphia (IAC 19-000907). Studies used 6- to 10-week old NOD-SCID-γc–/– (NSG) mice obtained from Jackson Laboratories or bred in-house under pathogen free conditions.

For medulloblastoma studies, Rcmb28 xenograft tumors were provided by Dr. Robert Weschler-Reya (Sanford Burnham), and 7316-4509 provided by the CBTN. Medulloblastoma xenografts were implanted stereotactically into the cerebellum of mice using the coordinates from lambda of: A/P -2.00mm, D/V 2.00mm, M/L -2.00mm. For thalamic DMG model, 7316-3058 was provided by the CBTN. This model was injected into the thalamus using the coordinates from bregma: A/P -1.00mm, D/V 3.50mm, M/L -0.80mm. Following engraftment, indwelling catheters to deliver intratumoral CAR T cells in the CNS were introduced using 26 gauge guide cannulas (C315GS-5/SPC, P1 Technologies), stereotactically placed and secured to the skull using screws (C212SG, P1 Technologies) and acrylic resin (Ortho-Jet, Lang). Catheters were placed at the same coordinates as the tumor cell placement. T cells were infused using 33 gauge internal cannulas (C315IS-5/SPC, P1 Technologies) placed into the guide cannula and delivered over 1 minute in a Hamilton syringe. All studies included 6-10 animals per arm.

Immunohistochemical analysis

Primary tumor samples, tissue microarrays and xenograft tumors from sacrificed animals were stained for GPC2 using immunohistochemistry as previously described,[23] by the Children's Hospital of Philadelphia Pathology Core laboratory. Staining for GPC2 was graded in a blinded fashion by a neuropathologist. Animals treated with CAR T cells had tumors excised and were also stained with H&E and human CD3 (A0452, Dako), in addition to GPC2. Photographs were taken using a Leica DM4000B.

Statistical analysis

All data generated was evaluated using Prism 8 (Graphpad). Comparison of groups for *GPC2* expression was completed using two-sided Mann-Whitney test or Kruskal-Wallis test. Correlation was calculated using two-tailed Pearson. Comparison of means for *in vitro* and *in vivo* CAR T cell data was completed using two-sided student t-test and 2-way ANOVA. P-values <0.05 were considered statistically significant. Data is generally presented as the mean ± SEM or as noted in the figure and figure legend. Number of samples or replicates is indicated in the results, figures and figure legends.

Acknowledgements

This research was conducted using data and samples made available by the Children's Brain Tumor Network. We thank the patients and families who generously donated their tumor specimens.

This work was supported in part by a St. Baldrick's Foundation-Stand Up to Cancer Dream Team Translational Research Grant (SU2C-AACR-DT-27-17). Stand Up to Cancer is a division of the Entertainment Industry Foundation. Research Grants are administered by the American Association for Cancer Research, the Scientific Partner of SU2C (J.B.F., J.M.M., K.R.B.). This work was also supported by a Hyundai Hope on Wheels Young Investigator Award (J.B.F), the Alex's Lemonade Stand Foundation (K.R.B.), by NCI K12 CA076931-19 (J.B.F.), NCI K08 CA230223 (K.R.B.), NCI U54 CA232568 (J.M.M.), NCI R35 CA220500 (J.M.M.), the Giulio D'Angio Endowed Chair (J.M.M.), Kortney Rose Foundation (J.B.F.), Grayson Saves Foundation (J.B.F.) and the EVAN Foundation (K.R.B.). K.R.B. is a Damon Runyon Physician-Scientist supported (in part) by the Damon Runyon Cancer Research Foundation (PST-07-16).

Author contributions

Conceptualization, J.B.F., D.M.B., A.C.R., J.M.M., and K.R.B.; Methodology, J.B.F., T.S., D.M.B., and K.R.B.; Software, J.L.R. and K.R.; Data Curation, J.L.R. and K.R.; Formal analysis, J.B.F.; Investigation, J.B.F., C.G., A.S.,C.B., M.L, S.B., and D.M.; Resources, R.W.R., K.K., A.C.R., J.M.M., and K.R.B.; Writing – Original Draft, J.B.F.; Writing – Review & Editing, J.B.F., J.L.R., C.B., K.K., J.M.M., and K.R.B.; Supervision, D.M.B., A.C.R., J.M.M., and K.R.B.; Funding Acquisition, J.B.F., P.B.S., A.C.R., J.M.M., and K.R.B.

References

1. Couzin-Frankel J. Cancer Immunotherapy. Science 2013;342:1432-3.

2. Almasbak H, Aarvak T, Vemuri MC. CAR T Cell Therapy: A Game Changer in Cancer Treatment. J Immunol Res 2016;2016:5474602.

3. Maude SL, Frey N, Shaw PA, et al. Chimeric antigen receptor T cells for sustained remissions in leukemia. N Engl J Med 2014;371:1507-17.

4. Fry TJ, Shah NN, Orentas RJ, et al. CD22-targeted CAR T cells induce remission in B-ALL that is naive or resistant to CD19-targeted CAR immunotherapy. Nature Medicine 2017;24:20.

5. Gardner R, Finney O, Smithers H, et al. CD19CAR T Cell Products of Defined CD4:CD8 Composition and Transgene Expression Show Prolonged Persistence and Durable MRD-Negative Remission in Pediatric and Young Adult B-Cell ALL. Blood 2016;128:219-.

6. First-Ever CAR T-cell Therapy Approved in U.S. Cancer Discovery 2017;7:OF1-OF.

7. Wagner J, Wickman E, DeRenzo C, Gottschalk S. CAR T Cell Therapy for Solid Tumors: Bright Future or Dark Reality? Mol Ther 2020;28:2320-39.

8. O'Rourke DM, Nasrallah MP, Desai A, et al. A single dose of peripherally infused EGFRvIII-directed CAR T cells mediates antigen loss and induces adaptive resistance in patients with recurrent glioblastoma. Science Translational Medicine 2017;9:eaaa0984.

9. Brown CE, Alizadeh D, Starr R, et al. Regression of Glioblastoma after Chimeric Antigen Receptor T-Cell Therapy. N Engl J Med 2016;375:2561-9.

10. Brown CE, Badie B, Barish ME, et al. Bioactivity and Safety of IL13Rα2-Redirected Chimeric Antigen Receptor $CD8^+$ T Cells in Patients with Recurrent Glioblastoma. Clinical Cancer Research 2015;21:4062-72.

11. Feins S, Kong W, Williams EF, Milone MC, Fraietta JA. An introduction to chimeric antigen receptor (CAR) T-cell immunotherapy for human cancer. American Journal of Hematology 2019;94:S3-S9.

12. Foster JB, Barrett DM, Karikó K. The Emerging Role of In Vitro-Transcribed mRNA in Adoptive T Cell Immunotherapy. Molecular Therapy 2019;27:747-56.

13. Foster JB, Choudhari N, Perazzelli J, et al. Purification of mRNA Encoding Chimeric Antigen Receptor Is Critical for Generation of a Robust T-Cell Response. Hum Gene Ther 2019;30:168-78.

14. Pardi N, Hogan MJ, Weissman D. Recent advances in mRNA vaccine technology. Current Opinion in Immunology 2020;65:14-20.

15. Barrett DM, Zhao Y, Liu X, et al. Treatment of advanced leukemia in mice with mRNA engineered T cells. Hum Gene Ther 2011;22:1575-86.

16. Singh N, Barrett DM, Grupp SA. Roadblocks to success for RNA CARs in solid tumors. Oncoimmunology 2014;3:e962974.

17. Morgan RA, Chinnasamy N, Abate-Daga D, et al. Cancer regression and neurological toxicity following anti-MAGE-A3 TCR gene therapy. J Immunother 2013;36:133-51.

18. Singh N, Liu X, Hulitt J, et al. Nature of tumor control by permanently and transiently modified GD2 chimeric antigen receptor T cells in xenograft models of neuroblastoma. Cancer Immunol Res 2014;2:1059-70.

19. Liu X, Jiang S, Fang C, et al. Novel T cells with improved in vivo anti-tumor activity generated by RNA electroporation. Protein & Cell 2017;8:514-26.

20. Beatty GL, O'Hara MH, Lacey SF, et al. Activity of Mesothelin-Specific Chimeric Antigen Receptor T Cells Against Pancreatic Carcinoma Metastases in a Phase 1 Trial. Gastroenterology 2018;155:29-32.

21. Ang WX, Li Z, Chi Z, et al. Intraperitoneal immunotherapy with T cells stably and transiently expressing anti-EpCAM CAR in xenograft models of peritoneal carcinomatosis. Oncotarget 2017;8:13545-59.

22. Beatty GL, Haas AR, Maus MV, et al. Mesothelin-specific chimeric antigen receptor mRNA-engineered T cells induce anti-tumor activity in solid malignancies. Cancer Immunol Res 2014;2:112-20.

23. Bosse KR, Raman P, Zhu Z, et al. Identification of GPC2 as an Oncoprotein and Candidate Immunotherapeutic Target in High-Risk Neuroblastoma. Cancer Cell 2017;32:295-309 e12.

24. Raman S, Buongervino SN, Lane MV, et al. The D3-GPC2-PBD antibody-drug conjugate is efficacious against neuroblastoma and small cell lung cancer via engagement of a conformational GPC2 epitope. Cell Reports Med 2021; in press.

25. Li N, Fu H, Hewitt SM, Dimitrov DS, Ho M. Therapeutically targeting glypican-2 via single-domain antibody-based chimeric antigen receptors and immunotoxins in neuroblastoma. Proc Natl Acad Sci U S A 2017;114:E6623-E31.

26. Li N, Torres MB, Spetz MR, et al. CAR T cells targeting tumor-associated exons of glypican 2 regress neuroblastoma in mice. Cell Reports Medicine 2021;2:100297.

27. Ijaz H, Koptyra M, Gaonkar KS, et al. Pediatric high-grade glioma resources from the Children's Brain Tumor Tissue Consortium. Neuro Oncol 2020;22:163-5.

28. Wenger A, Larsson S, Danielsson A, et al. Stem cell cultures derived from pediatric brain tumors accurately model the originating tumors. Oncotarget 2017;8.

29. Vik-Mo EO, Sandberg C, Olstorn H, et al. Brain tumor stem cells maintain overall phenotype and tumorigenicity after in vitro culturing in serum-free conditions. Neuro-Oncology 2010;12:1220-30.

30. Theruvath J, Sotillo E, Mount CW, et al. Locoregionally administered B7-H3-targeted CAR T cells for treatment of atypical teratoid/rhabdoid tumors. Nature Medicine 2020.

31. Mount CW, Majzner RG, Sundaresh S, et al. Potent antitumor efficacy of anti-GD2 CAR T cells in H3-K27M(+) diffuse midline gliomas. Nat Med 2018;24:572-9.

32. Curtin SC, Minino AM, Anderson RN. Declines in Cancer Death Rates Among Children and Adolescents in the United States, 1999-2014. NCHS Data Brief 2016:1-8.

33. Bjerke L, Mackay A, Nandhabalan M, et al. Histone H3.3 Mutations Drive Pediatric Glioblastoma through Upregulation of MYCN. Cancer Discovery 2013;3:512-9.

34. Wang J, Merino DM, Light N, et al. Myc and Loss of p53 Cooperate to Drive Formation of Choroid Plexus Carcinoma. Cancer Research 2019;79:2208-19.

35. Schutsky K, Song DG, Lynn R, et al. Rigorous optimization and validation of potent RNA CAR T cell therapy for the treatment of common epithelial cancers expressing folate receptor. Oncotarget 2015;6:28911-28.

36. Donovan LK, Delaidelli A, Joseph SK, et al. Locoregional delivery of CAR T cells to the cerebrospinal fluid for treatment of metastatic medulloblastoma and ependymoma. Nature Medicine 2020.

37. Brown CE, Aguilar B, Starr R, et al. Optimization of IL13Rα2-Targeted Chimeric Antigen Receptor T Cells for Improved Anti-tumor Efficacy against Glioblastoma. Molecular Therapy 2018;26:31-44.

38. Shapiro JA SC, Bethell CJ, Gaonkar KS, Zhu Y, Brown MA, et al. An open pediatric brain tumor atlas. Manubot [Internet] 2020:https://alexslemonade.github.io/OpenPBTA-manuscript/v/7207b5942e7c5ee8a363f2cc54c4a78ec06f810e/.

39. Harenza JL, Diamond MA, Adams RN, et al. Transcriptomic profiling of 39 commonly-used neuroblastoma cell lines. Scientific Data 2017;4:170033.

40. Campeau E, Ruhl VE, Rodier F, et al. A versatile viral system for expression and depletion of proteins in mammalian cells. PLoS One 2009;4:e6529.

41. Carpenito C, Milone MC, Hassan R, et al. Control of large, established tumor xenografts with genetically retargeted human T cells containing CD28 and CD137 domains. Proc Natl Acad Sci U S A 2009;106:3360-5.

42. Zheng Z, Chinnasamy N, Morgan RA. Protein L: a novel reagent for the detection of Chimeric Antigen Receptor (CAR) expression by flow cytometry. Journal of Translational Medicine 2012;10:29.

Figures Legends

Figure 1. *GPC2* is expressed in pediatric brain tumors.

(**A**) *GPC2* RNA sequencing data across OpenPBTA pediatric brain tumors cohorts.

(**B**) Using a cut-off value of 10 TPM, percentage of tumors in OpenPBTA dataset with high expression of *GPC2*.

(**C**) RNA sequencing of *GPC2* expression in medulloblastoma, high grade glioma, and embryonal tumor subtypes.

(**D**) Summary of tumor histotypes with chromosome 7q gain.

(**E**) *GPC2* expression stratified by chromosome 7q status.

(**F**) Correlation of *MYCN* and *GPC2* expression across all pediatric brain tumor samples (top), medulloblastomas (middle), and high-grade gliomas (bottom).

(**G**) *GPC2* expression at primary diagnosis and recurrence across all pediatric brain tumors (top), medulloblastomas (bottom left), and high-grade gliomas (bottom right).

(**H**) *GPC2*, *CD133*, *SOX2,* and *OLIG2* expression from primary tumor-derived adherent (FBS) or suspension cell lines (serum free media).

TPM = transcripts per million, NOS = not otherwise specified, ETMR = embryonal tumor with multilayered rosettes, CPC = choroid plexus carcinoma, DMG = diffuse midline glioma, HGG = high grade glioma, LGG = low grade glioma, DNET = dysembryoplastic neuroepithelial tumor, ATRT = atypical teratoid rhabdoid tumor, GCT = germ cell tumor, and CPP = choroid plexus papilloma. Individual cases indicated by dots, median indicated by line in **A, C** and **H**. Data in **E** displayed as median with 95% confidence interval. ****, $p<0.0001$; **, $p<0.01$; *, $p<0.05$; ns, not significant.

Figure 2. GPC2 protein is expressed on the surface of pediatric brain tumors

(**A**) GPC2 IHC of primary HGGs (n=67) with representative GPC2 IHC staining examples (left) and GPC2 IHC summary (right).

(**B**) GPC2 IHC showing strongly positive staining in additional brain tumor histotypes including H3 G35 mutant HGG, medulloblastoma, ETMR, pineoblastoma, HGNET-BCOR, and CNS embryonal tumor NOS.

(**C**) GPC2 flow cytometry representative histograms of HGG and medulloblastoma cell lines. Red shaded curves indicate D3-GPC2-IgG1-PE staining, non-shaded curves indicate isotype control. SMS-SAN shown as neuroblastoma positive control and T cells as negative control.

(**D**) Summary of the relative quantification of GPC2 molecules per cell from flow cytometry of HGG and medulloblastoma cell lines (n=11). Data is represented as mean ± SEM of 3 independent experiments.

(**E**) GPC2 Western blot of a panel of medulloblastoma and HGG cell lines (n=9). SMS-SAN also presented as neuroblastoma positive control.

HGG, high grade glioma; ETMR, embryonal tumor with multilayered rosettes; HGNET-BCOR, high grade neuroepithelial tumor with BCOR alteration.

Figure 3. D3-binder based GPC2-directed mRNA CARs specifically bind GPC2 and are transiently expressed on T cells.

(**A**) Schematic of GPC2 CAR constructs.

(**B**) Flow cytometry representative histograms of GPC2 specific binding by GPC2 CAR T cell constructs. Red line is CAR T cell, grey line is untransfected T cell control.

(**C**) Flow cytometry representative histograms GPC2 CAR persistence on T cells. Red line represents day 1 post-transfection, blue line represents day 3, orange line day 5, and green line day 7. Grey line is untransfected T cell control.

(**D**) Cell surface expression of negative checkpoint regulators PD1, Lag3 and Tim3 quantified with flow cytometry at day 4 post-transfection. Data is represented as mean ± SEM of three independent experiments.

V_H, variable heavy chain; V_L, variable light chain; T_M, transmembrane domain; BB, 41-BB co-stimulatory domain; 3z, CD3ζ co-stimulatory domain; MFI, mean fluorescence intensity; ns, not significant. Graphics in **A** created with BioRender.com.

Figure 4. GPC2-directed CAR T cells produce robust cytotoxicity in neuroblastoma cell line models.

(**A, B**) GPC2-directed CAR T cells co-incubated with both high (A) and low (B) GPC2 expressing cell lines on an RT-CES.

(**C**) Cytokine expression measured 24 hours after co-incubation of neuroblastoma and GPC2-directed CAR T cells.

E:T, Effector to target ratio. Data is shown as mean ± SEM from a representative experiment with each experiment being done two to four independent times.

Figure 5. GPC2-directed CAR T cells produce robust cytotoxicity in pediatric brain tumor cell line models.

(**A**) GPC2-directed CAR T cells co-incubated with medulloblastoma (DAOY), HGG (7316-913), and DMG (7316-5335) cell lines. E:T ratio is 5:1.

(**B**) GPC2 CAR T cells co-inbuated with medulloblastoma (7316-4509), HGG (7316-24), and DMG (7316-3058) cell lines with cytotoxicity measured using a luminescence assay at 48 hours.

(**C**) Cytokine levels measured 24 hours after co-incubation of GPC2 CAR T cells with each cell line.

Data is shown as mean ± SEM from a representative experiment with each experiment being done two to four independent times.

Figure 6. GPC2-directed CAR T cells mediate antitumor responses and prolong survival in pediatric brain tumors *in vivo*

(**A**) Quantification of bioluminescence of the orthotopic group 4 medulloblastoma xenograft 7316-4509 treated with either GPC2 or CD19-directed mRNA CAR T cells. Doses indicated by arrows on graph. Data displayed as mean ± SEM, n= 10 mice per arm.

(**B**) Quantification of bioluminescence of the orthotopic group 3 medulloblastoma xenograft Rcmb28 treated with either GPC2 or CD19-directed mRNA CAR T cells. Doses indicated by arrows on graph. Data displayed as mean ± SEM, n= 6-8 mice per arm.

(**C**) Overall survival of mice implanted with thalamic DMG xenograft 7316-3058 treated with six repeated doses of 2 x 10^6 CAR T cells. N= 7 nice per arm.

(**D**) IHC of murine brains of a representative mouse per group collected at study endpoint from medulloblastoma xenograft 7316-4509 experiment in **A**. Human nuclei stain to identify human tumor cells, GPC2 staining for tumor identification and expression, CD3 stain to identify CAR T cells. Scale bar is 2000μm at low power, 250μm at insert.

****, $p<0.0001$; **, $p<0.01$; *, $p<0.05$; ns, not significant.

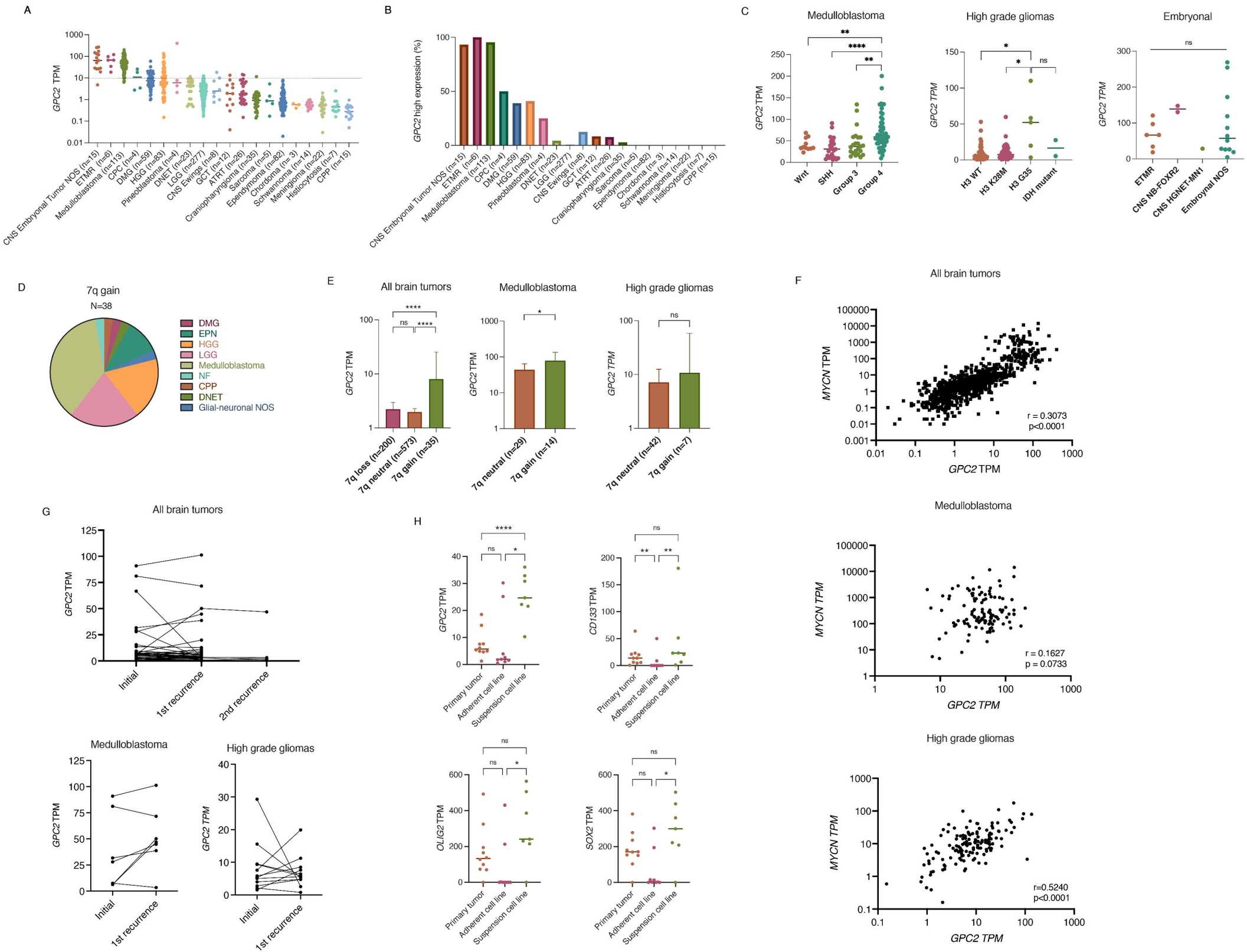
A
GPC2 TPM
CNS Embryonal Tumor NOS (n=15)
ETMR (n=6)
Medulloblastoma (n=113)
CPC (n=4)
DMG (n=59)
HGG (n=83)
Pineoblastoma (n=4)
DNET (n=23)
LGG (n=277)
CNS Ewings (n=8)
GCT (n=12)
ATRT (n=26)
Craniopharyngioma (n=35)
Sarcoma (n=5)
Ependymoma (n=82)
Chordoma (n= 3)
Schwannoma (n=14)
Meningioma (n=22)
Histiocytosis (n=7)
CPP (n=15)
B
GPC2 high expression (%)
C
Medulloblastoma
High grade gliomas
Embryonal
Wnt
SHH
Group 3
Group 4
H3 WT
H3 K28M
H3 G35
IDH mutant
ETMR
CNS NB-FOXR2
CNS HGNET-MN1
Embroynal NOS
D
7q gain
N=38
DMG
EPN
HGG
LGG
Medulloblastoma
NF
CPP
DNET
Glial-neuronal NOS
E
All brain tumors
Medulloblastoma
High grade gliomas
GPC2 TPM
7q loss (n=200)
7q neutral (n=573)
7q gain (n=35)
7q neutral (n=29)
7q gain (n=14)
7q neutral (n=42)
7q gain (n=7)
F
All brain tumors
MYCN TPM
GPC2 TPM
r = 0.3073
p<0.0001
Medulloblastoma
r = 0.1627
p = 0.0733
High grade gliomas
r=0.5240
p<0.0001
G
All brain tumors
Initial
1st recurrence
2nd recurrence
Medulloblastoma
High grade gliomas
H
Primary tumor
Adherent cell line
Suspension cell line
CD133 TPM
OLIG2 TPM
SOX2 TPM

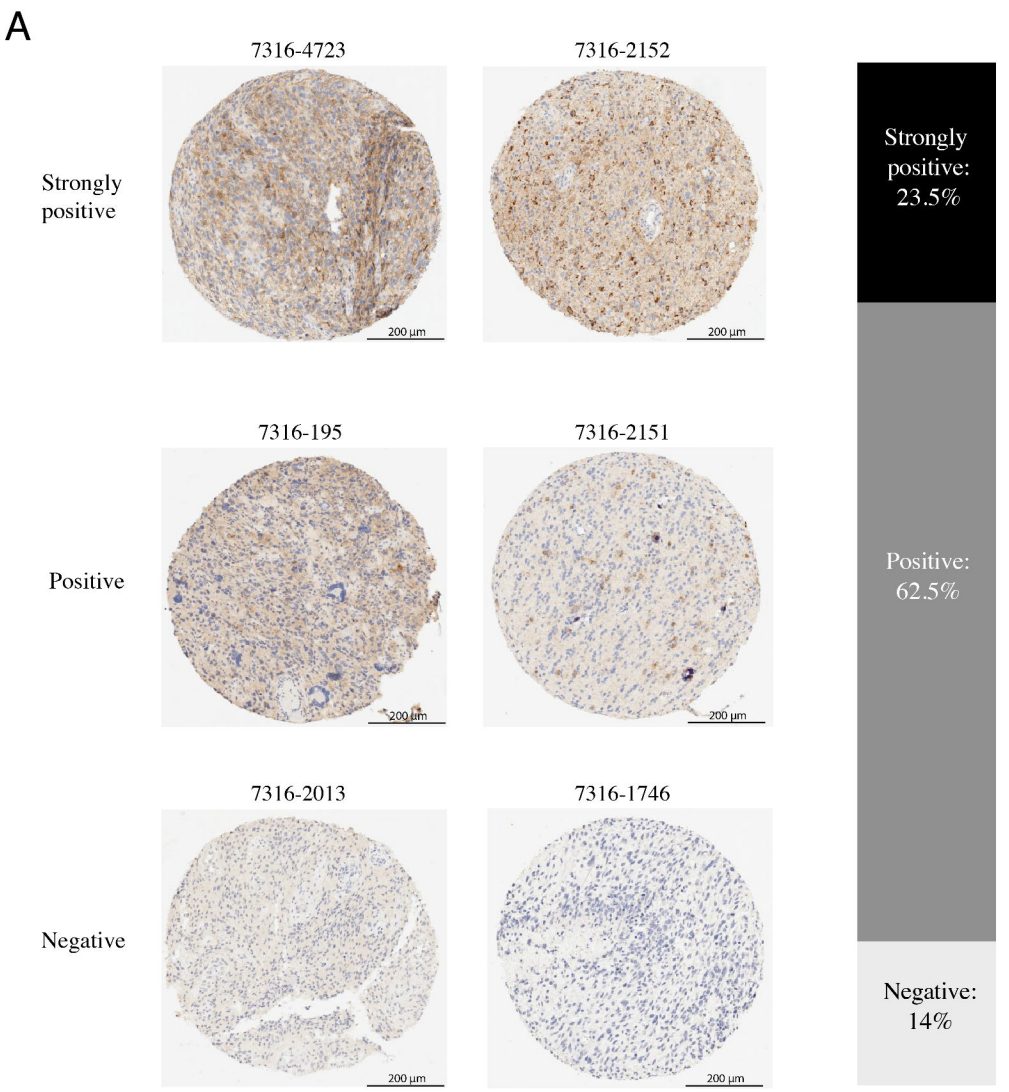
A
7316-4723
7316-2152
Strongly positive
7316-195
7316-2151
Positive
7316-2013
7316-1746
Negative
200 µm
Strongly positive: 23.5%
Positive: 62.5%
Negative: 14%

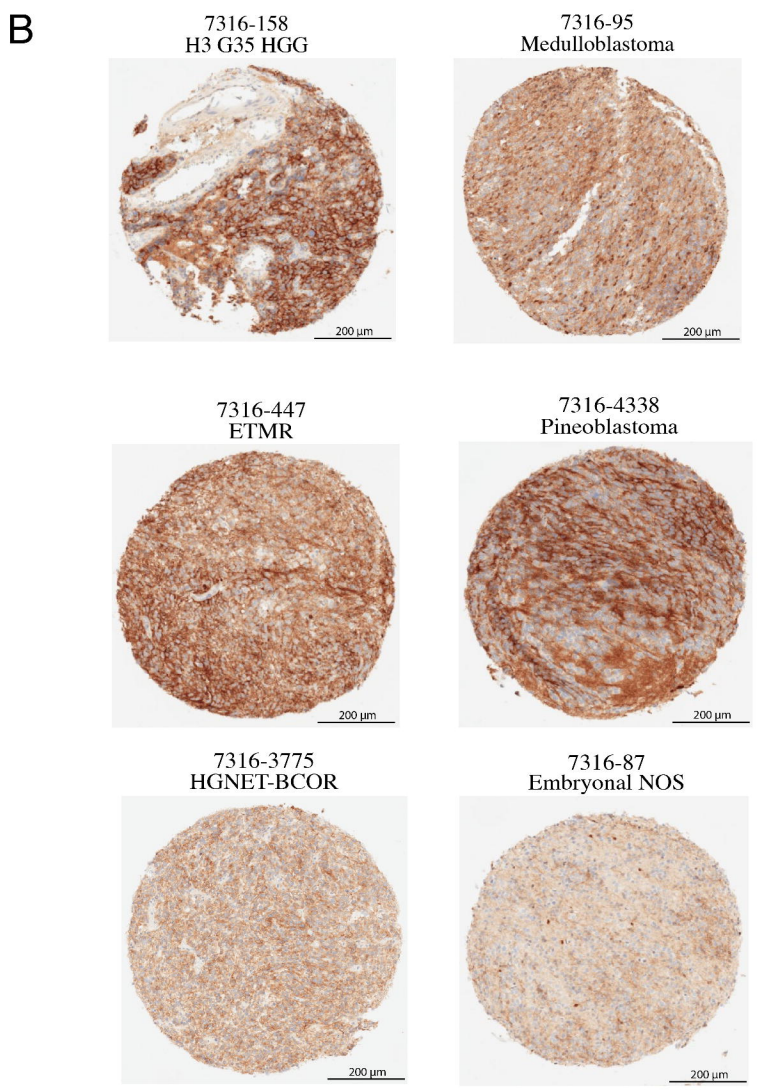
B
7316-158
H3 G35 HGG
7316-95
Medulloblastoma
7316-447
ETMR
7316-4338
Pineoblastoma
7316-3775
HGNET-BCOR
7316-87
Embryonal NOS
200 µm

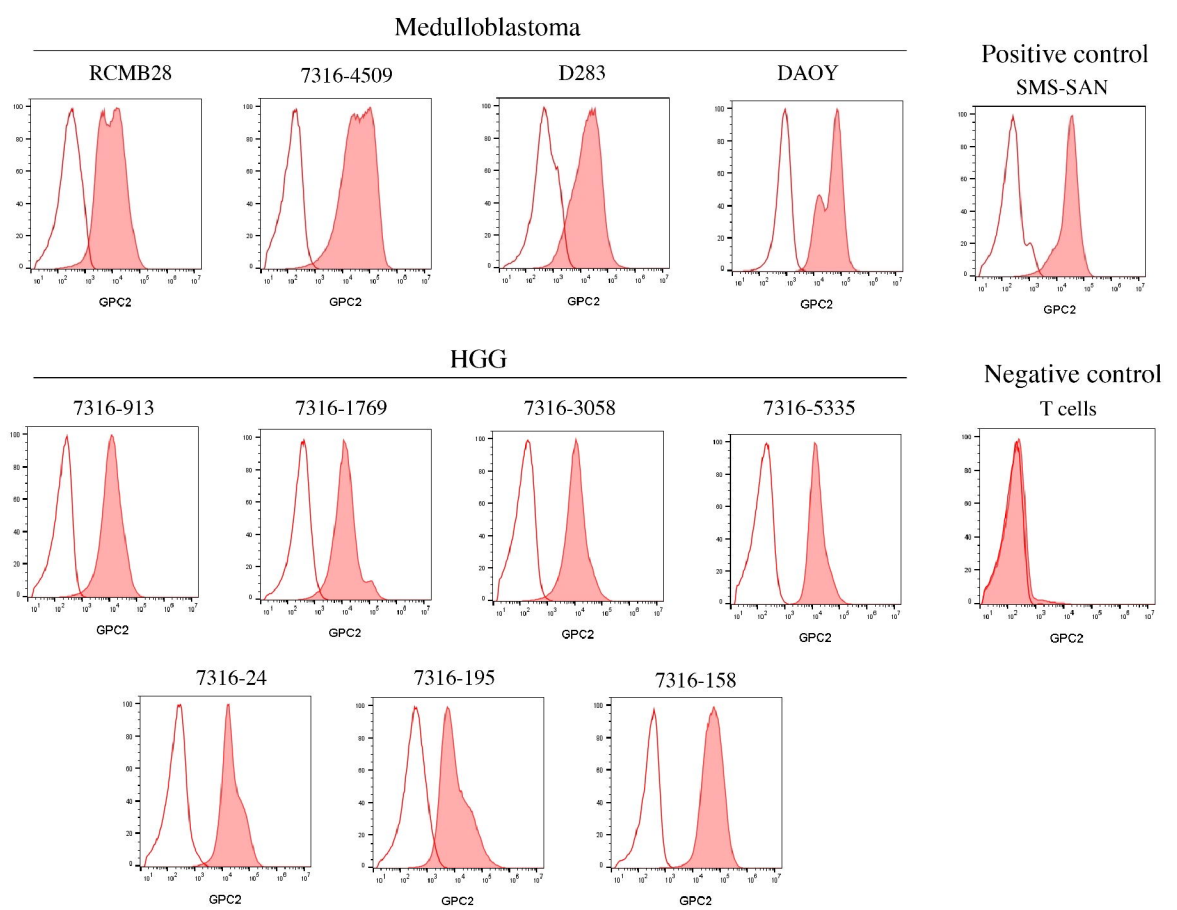
C
Medulloblastoma
RCMB28
7316-4509
D283
DAOY
Positive control
SMS-SAN
HGG
7316-913
7316-1769
7316-3058
7316-5335
Negative control
T cells
7316-24
7316-195
7316-158
GPC2

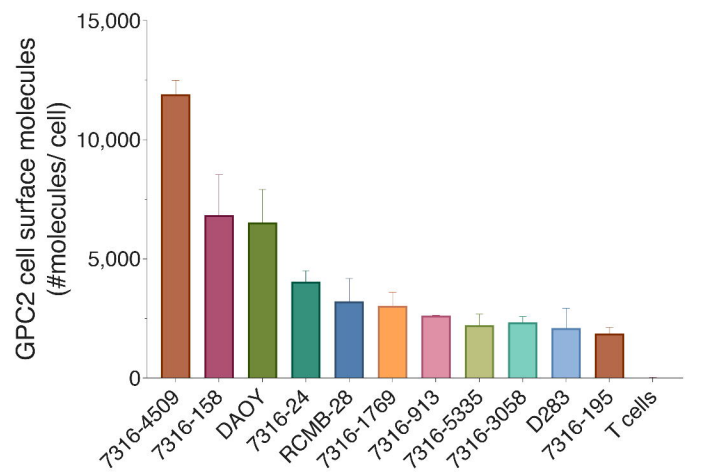
D
GPC2 cell surface molecules (#molecules/ cell)
15,000
10,000
5,000
0
7316-4509
7316-158
DAOY
7316-24
RCMB-28
7316-1769
7316-913
7316-5335
7316-3058
D283
7316-195
T cells

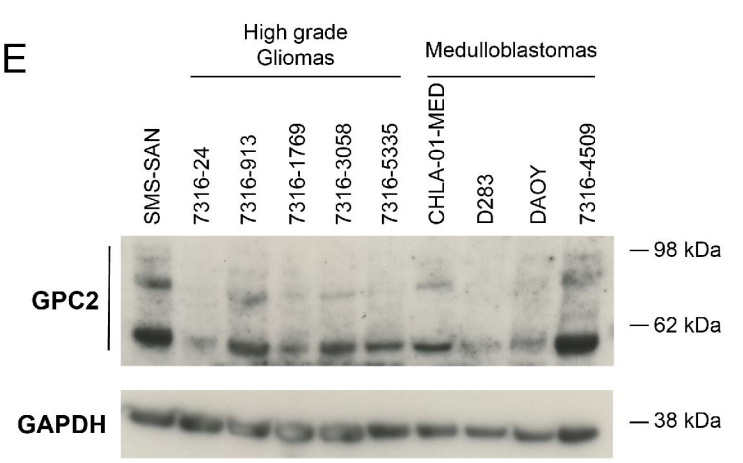
E
High grade Gliomas
Medulloblastomas
SMS-SAN
7316-24
7316-913
7316-1769
7316-3058
7316-5335
CHLA-01-MED
D283
DAOY
7316-4509
GPC2
GAPDH
98 kDa
62 kDa
38 kDa

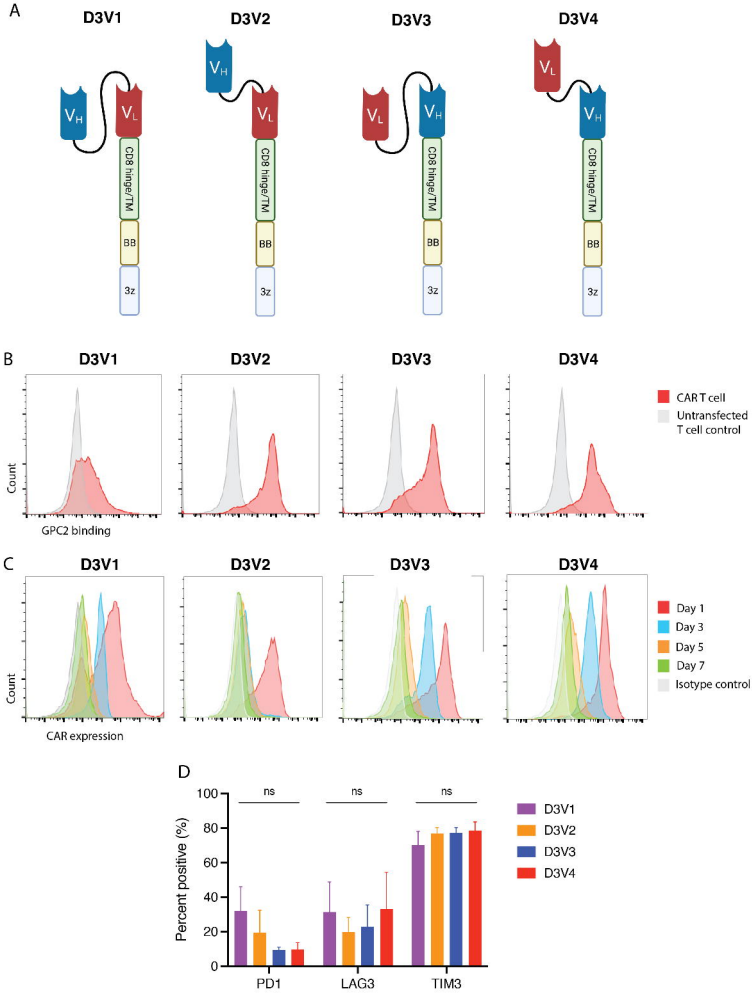
A
D3V1
D3V2
D3V3
D3V4
VH
VL
CD8 hinge/TM
BB
3z
B
Count
GPC2 binding
CAR T cell
Untransfected T cell control
C
CAR expression
Day 1
Day 3
Day 5
Day 7
Isotype control
D
Percent positive (%)
ns
PD1
LAG3
TIM3

A

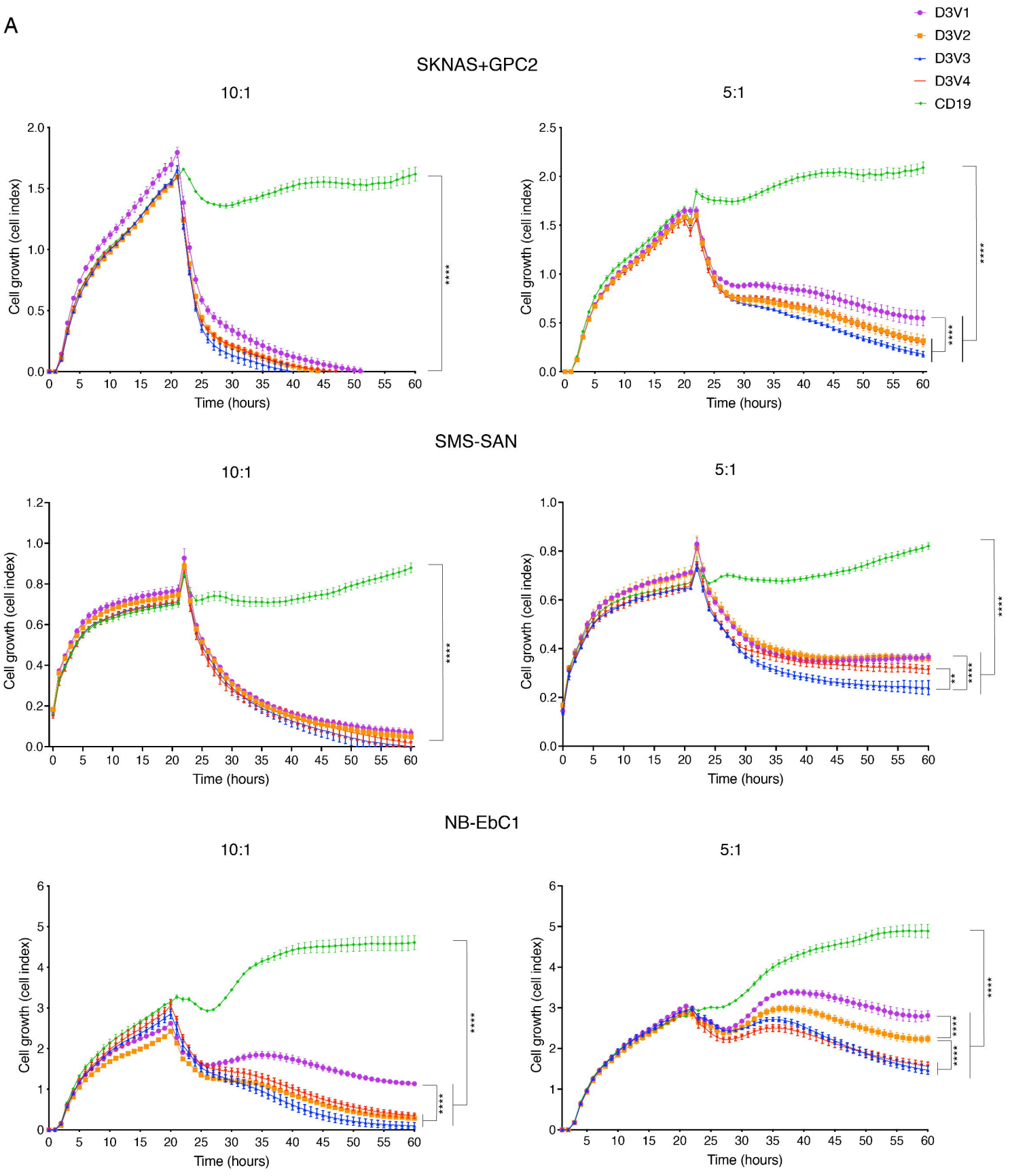
D3V1
D3V2
D3V3
D3V4
CD19
SKNAS+GPC2
10:1
5:1
SMS-SAN
10:1
5:1
NB-EbC1
10:1
5:1
Cell growth (cell index)
Time (hours)
****
**

B

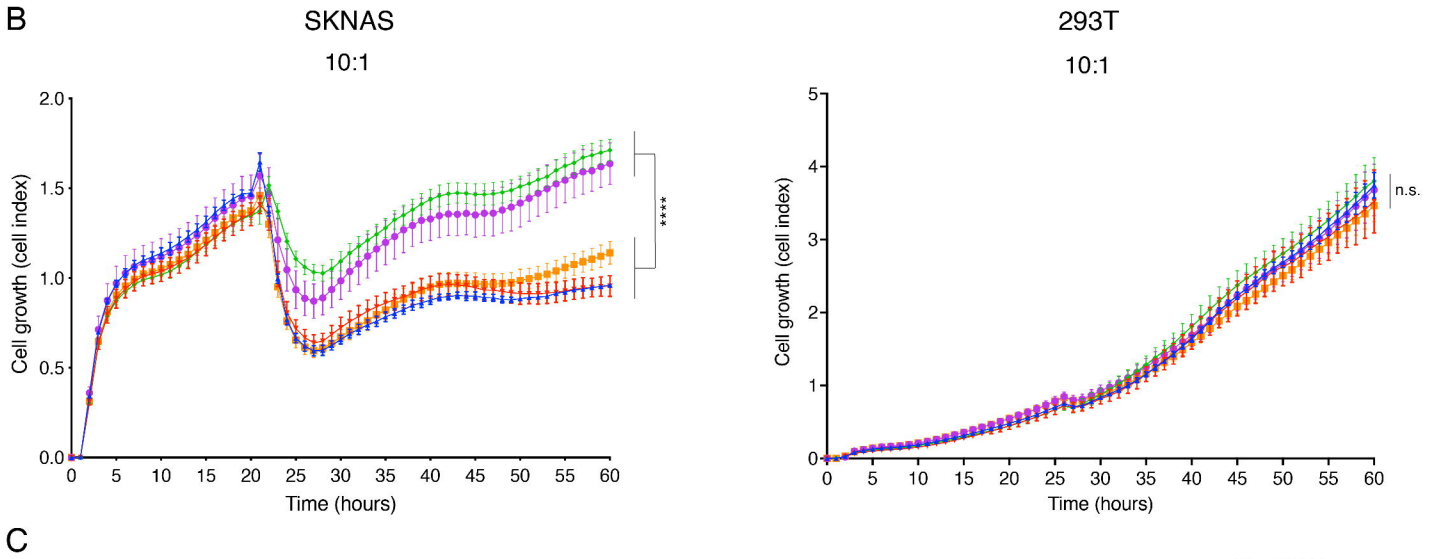
SKNAS
10:1
293T
10:1
Cell growth (cell index)
Time (hours)
****
n.s.

C

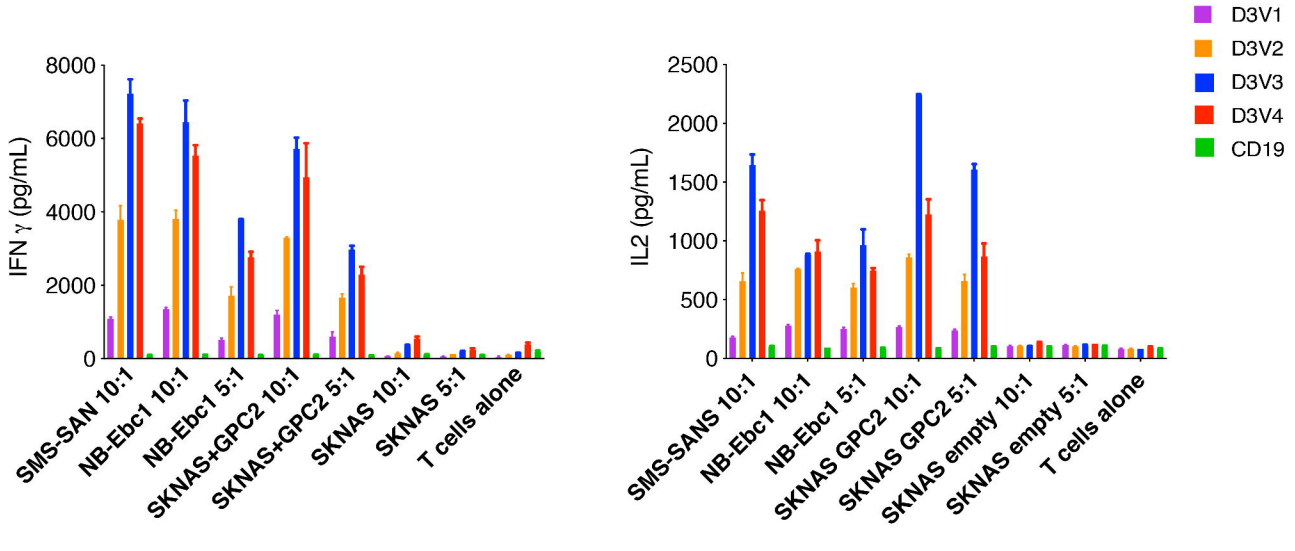
D3V1
D3V2
D3V3
D3V4
CD19
IFN γ (pg/mL)
IL2 (pg/mL)
SMS-SAN 10:1
NB-Ebc1 10:1
NB-Ebc1 5:1
SKNAS+GPC2 10:1
SKNAS+GPC2 5:1
SKNAS 10:1
SKNAS 5:1
T cells alone
SMS-SANS 10:1
NB-Ebc1 10:1
NB-Ebc1 5:1
SKNAS GPC2 10:1
SKNAS GPC2 5:1
SKNAS empty 10:1
SKNAS empty 5:1
T cells alone

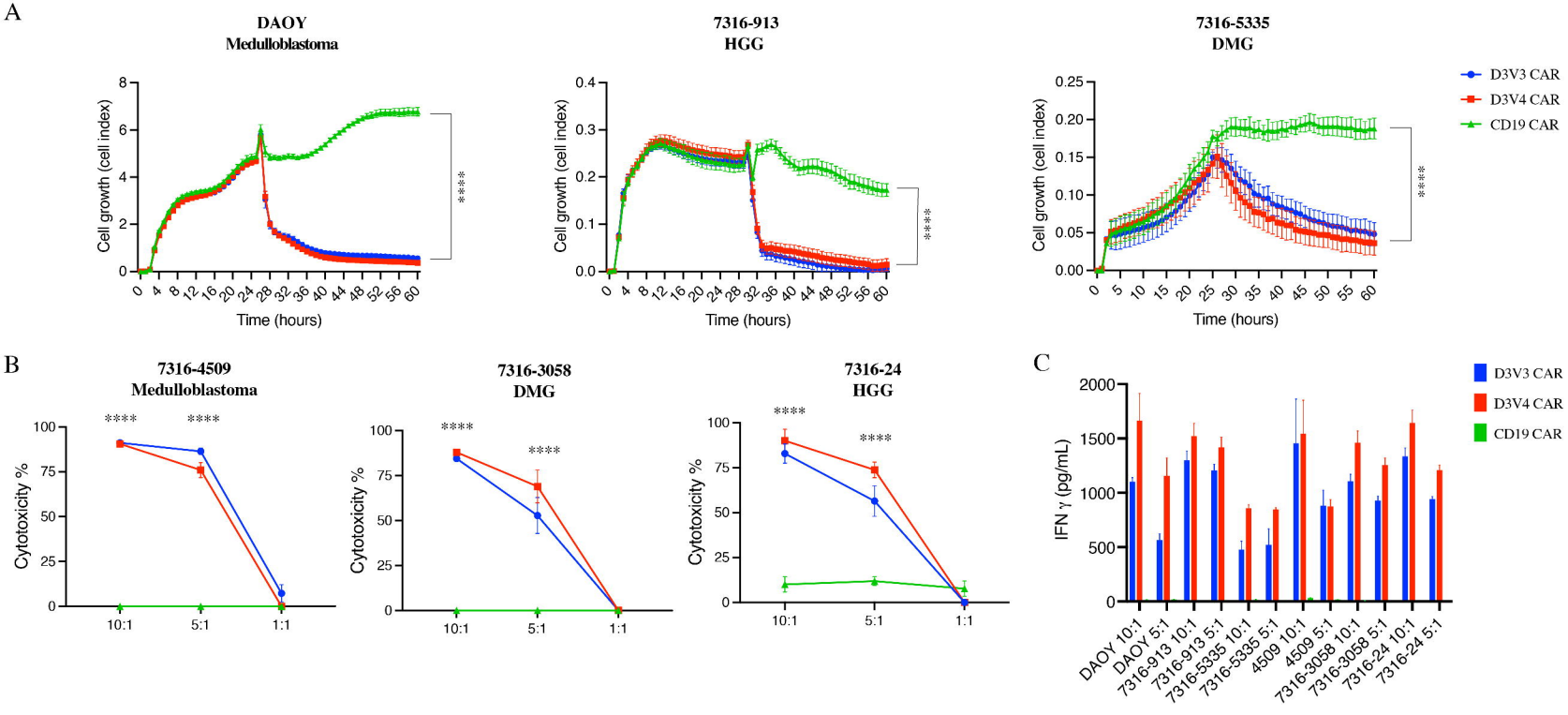
A
DAOY
Medulloblastoma
7316-913
HGG
7316-5335
DMG
Cell growth (cell index)
Time (hours)
****
D3V3 CAR
D3V4 CAR
CD19 CAR
B
7316-4509
Medulloblastoma
7316-3058
DMG
7316-24
HGG
Cytotoxicity %
10:1
5:1
1:1
C
IFN γ (pg/mL)
DAOY 10:1
DAOY 5:1
7316-913 10:1
7316-913 5:1
7316-5335 10:1
7316-5335 5:1
4509 10:1
4509 5:1
7316-3058 10:1
7316-3058 5:1
7316-24 10:1
7316-24 5:1

A

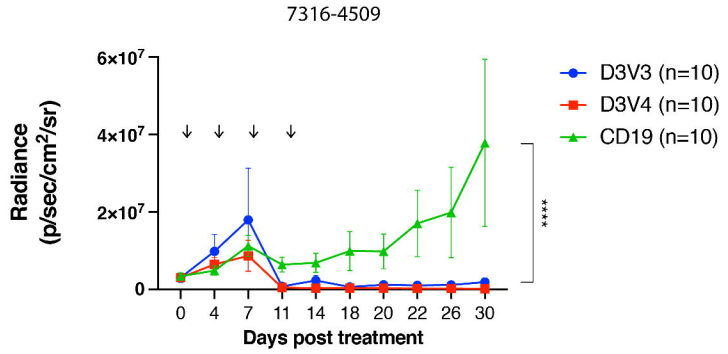
7316-4509
Radiance (p/sec/cm²/sr)
6×10⁷
4×10⁷
2×10⁷
0
0 4 7 11 14 18 20 22 26 30
Days post treatment
D3V3 (n=10)
D3V4 (n=10)
CD19 (n=10)
****

B

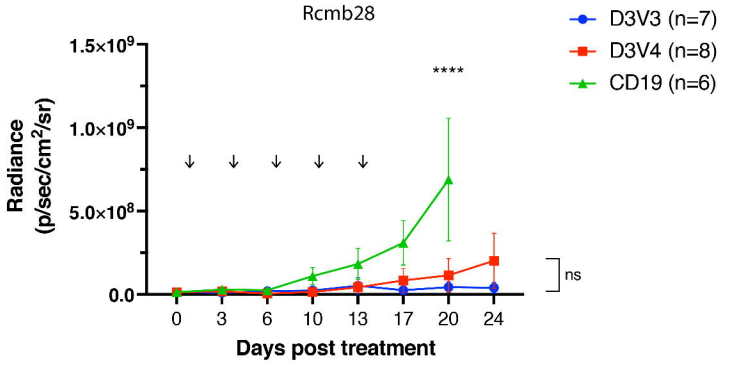
Rcmb28
Radiance (p/sec/cm²/sr)
1.5×10⁹
1.0×10⁹
5.0×10⁸
0.0
0 3 6 10 13 17 20 24
Days post treatment
D3V3 (n=7)
D3V4 (n=8)
CD19 (n=6)
****
ns

D

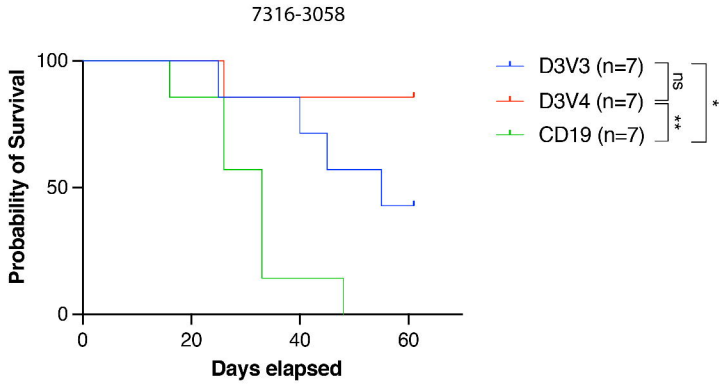
7316-3058
Probability of Survival
100
50
0
0 20 40 60
Days elapsed
D3V3 (n=7)
D3V4 (n=7)
CD19 (n=7)
ns
**
*

C

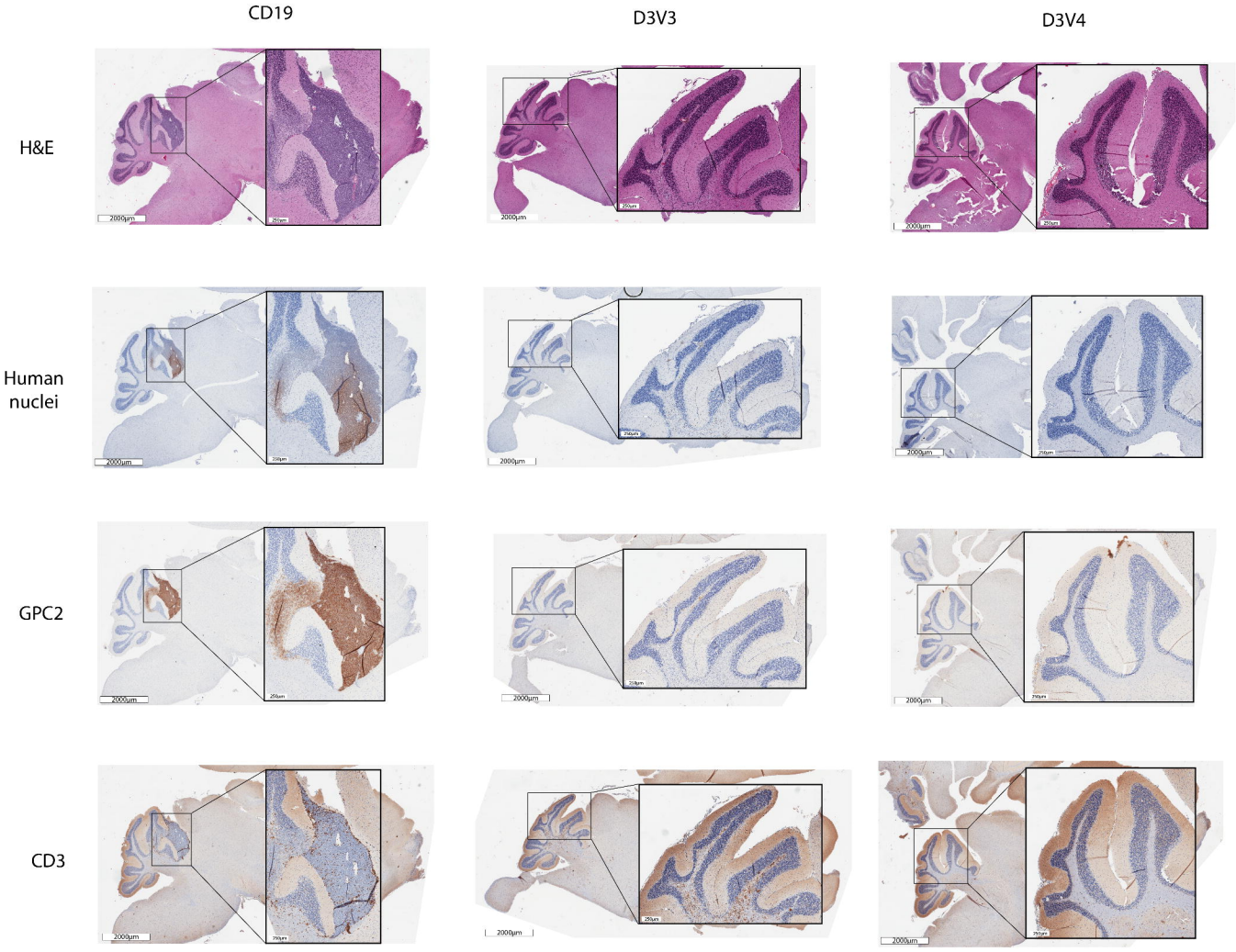
CD19
D3V3
D3V4
H&E
Human nuclei
GPC2
CD3